Local Mobility Anchoring for Seamless Handover in Coordinated Small Cells

Ravikumar Balakrishnan and **Ian F. Akyildiz**

Broadband Wireless Networking Laboratory
School of Electrical and Computer Engineering, Georgia Institute of Technology, Atlanta, GA 30332, USA.
Email: {rbalakrishnan6,ian}@ece.gatech.edu

***Abstract*—Small cells are redefining the traditional cellular system concepts. Coordination among small cells offers several benefits in terms of utilizing existing network infrastructure to support advanced interference management, mobility management as well as self-organizing (SON) functions. In this work, the problem of handover management is studied. The coordination between small cells is generally not considered in many existing handover management solutions resulting in increased handover cost, session interruption time and core network overload. To this end, a novel local anchor-based architecture for coordinated small cells is proposed in this paper based on which three handover schemes are presented. A mathematical framework is developed to analyze the performance of the proposed schemes and Markov models are utilized to obtain closed-form expressions for the key handover parameters including handover cost and session interruption time. Numerical results indicate savings of about 60% in the signaling cost, about 50% in the data forwarding cost and more importantly about 80% in the handover interruption time compared to existing schemes based on coordinated small cells.**

I. Introduction

THE rapidly growing need of mobile wireless data and services has resulted in tremendous advances in mobile networks both at the radio access and the network management technologies. In this regard, cellular networks are undergoing a major transformation with the existing macrocell coverage area underlaid with a number of low-powered small cell base stations to improve the overall system capacity. The emergence of this multi-layered approach requires a revision of many of the major enabling technologies including interference management and mobility management as pointed out in the Rel-12 of 3GPP LTE-Advanced systems [1]. In particular, the presence of a number of small cells underlaid within a macrocell layer causes frequent handovers from one cell to another for mobile users with an active session. In order to ensure seamless connectivity for the users, it is necessary to efficiently handle these frequent handovers [2].

Coordination among a set of small cells is ideal for small cell deployments in scenarios such as airports, malls, auditoriums and large office buildings. In fact, there are several standardization and industry efforts for enterprise small cells targeted for the above scenarios. This coordination enables achieving improved interference management, mobility management as well as self-organizing (SON) functions by utilizing the underlying network infrastructure. Specifically for mobility management, this coordination can also play a significant role in the following ways. First, it can enable scalable small cell deployments by minimizing the load on the core network during handovers. Furthermore, since the small cells incorporate different backhaul technologies including internet, microwave LOS, etc, coordination among small cells can help overcome potential backhaul issues of long latency and operating costs involved for signaling and data interaction during handovers. However, it must be mentioned that coordinated small cells also place some constraints such as requiring a network infrastructure with high-speed links.

Several existing work on handover management aim to minimize the key parameters of handover costs, interruption time. Local anchor-based mobility management schemes were studied in [3] for optimizing paging and registration updates. In [4], new architectures have been proposed to move the mobility anchor point closer to the base stations. However, incorporating these new architectures require redefining the security key mechanisms and signaling flow among other modifications. In [5], the authors propose a fast handover scheme. Nevertheless, this scheme does not provide significant savings on handover costs or the core network load. In [6], an X2-based data forwarding scheme analogous to the pointer forwarding technique is proposed.

In this work, we consider the case of coordinated small cells and propose a novel local anchor-based architecture for providing enhanced support for handover management. The contributions of the paper are summarized as follows:

- We propose novel handover schemes based on the local anchor-based architecture for coordinated small cells.
- We analytically model a cluster of small cells to study the mobility behaviour of users.
- We provide closed-form expressions for handover cost, handover interruption time under the proposed handover schemes.
- We present the numerical results highlighting the performance gains of over 80% reduction in the session interruption time and more than 50% reduction in the handover costs.

The rest of this paper is organized as follows. The local anchor-based architecture and the proposed handover mechanisms are presented in Sec. II. In Sec. III, the analytical model developed to study the mobility behavior of users is described. In Sec. IV, the closed-from expressions for several handover performance metrics are derived. Numerical results are presented in Sec. V. Finally, the main conclusions are summarized in Sec. VI.

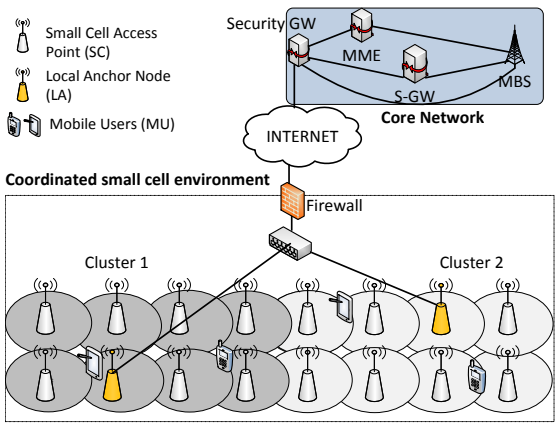

Fig. 1: Local anchor based handover architecture

II. Local Anchor-based Handover Management

In this section, we first motivate the need for a new handover architecture for coordinated small cells and then describe our proposed local anchor-based handover architecture.

A. Motivation

The handover procedure for 3GPP LTE-A systems utilizing the direct interface (X2 interface) between small cells is divided into three phases: (i) handover preparation, (ii) handover execution, and (iii) handover completion. We refer the readers to [7] for a detailed explanation of the handover procedure.

The key observation from the above X2-based handover procedure is that the mobility anchor for the handover is the core network (particularly the MME). This gives the intuition that the backhaul for the small cells needs to have the key characteristics of low-latency and high reliability. The total downlink interruption time for a normal handover procedure is computed as $\max(\mathbf{18.5ms}, \mathbf{T_p})$ in [8] where T_p is the path switching delay. This confirms that the backhaul latency (to perform path switching) should not exceed few tens of milliseconds. However, many of the small cell technologies cannot meet this stringent backhaul latency requirements. Therefore, we advocate the use of local mobility anchoring that can satisfy the objectives of minimizing total handover costs, handover interruption time and core network load.

B. Local Anchor-based Architecture

With the above core objectives in mind, we propose a local anchor-based (LA-based) architecture for a set of coordinated small cells. We divide a large array of small cells into several clusters where each cluster contains a subset of small cells. The local anchor-based architecture is shown in Fig. 1. One of the small cells in a cluster is chosen as the local anchor (LA). The small cells inside a cluster are assumed to connect to a local network. The local anchors maintain connection with the IP gateway of the local network which is connected to the Mobile Core Network (CN) through a firewall and public internet. The main advantage of the LA-based architecture is that handover mechanisms can be proposed that utilize the **LA as the mobility anchor** therefore minimizing the handover interruption as well as the associated costs.

EPS Bearer ID	SC Info			CN Info		
	SC S1AP ID	Transport Layer Address	GTP TEID of SC	CN S1AP ID	Transport Layer Address	GTP TEID of CN

Fig. 2: Local anchor registration table

The functions of the LA are summarized as follows:

- *Concentrator of traffic between SCs and CN*: In this sense, the LA performs proxy tunnelling function for the interface between SCs in its cluster and the CN (S1 interface, in case of LTE-A). The LA is also capable of proxy X2 functions to enable handover to SCs belonging to other clusters or to macrocell base station (MBS). In order to achieve the proxy tunnelling between SCs and CN, the LA maintains a local anchor registration table **(LART)**. This is shown in Fig. 2. The LART contains the data and signaling plane end point addresses. This is also enabled by maintaining S1 security over two hops between for CN $\Leftrightarrow$ LA and LA $\Leftrightarrow$ SC links.
- *Local Mobility Anchor for handover between other SCs*: The LA acts as a local mobility anchor for the users performing handover between SCs in its cluster. The LA is able to perform local path switching without affecting the established procedures and only forwards the path switch request to the CN once certain conditions are met.

Using the local anchor based-architecture, the handover mechanism are outlined in the next subsections.

C. Local path switching-based handover

Originally, the target SC of an MS undergoing handover sends a path switch request message to the core network to indicate the completion of handover and to enable the CN to switch the downlink path for the MS towards the target SC. More importantly, the path switching also enables the CN to generate new keys for securing the SC $\Longleftrightarrow$ MS interface. A detailed explanation of the key management is available in [9]. This new key also helps overcome issues concerned with forward key separation, i.e., once the target SC receives the new key (through vertical key derivation) in path switch request ack from the MME, the previous SC cannot decode the keys of the target SC.

If the path switching is not performed, then the target SC will continue to use the key derived by the previous SC (horizontal key derivation) from which the MS handed over from. However, due to longer backhaul latency and frequent handover in small cells, the **path switch request ack** from the MME is not always received in time to achieve the best case of 2-hop backward key separation. At the same time, performing the path switch with the core network seriously degrades the handover performance.

In this scheme, we advocate the use of **local path switching** for SCs belonging to the same cluster for upto ν number of handovers for a given MS. To achieve this, the LA maintains a counter value for each user until its session ends and performs path switching with the CN, only when the counter value is equal to ν. Then the LA resets the counter and continues incrementing until the session for the MS ends. Therefore,

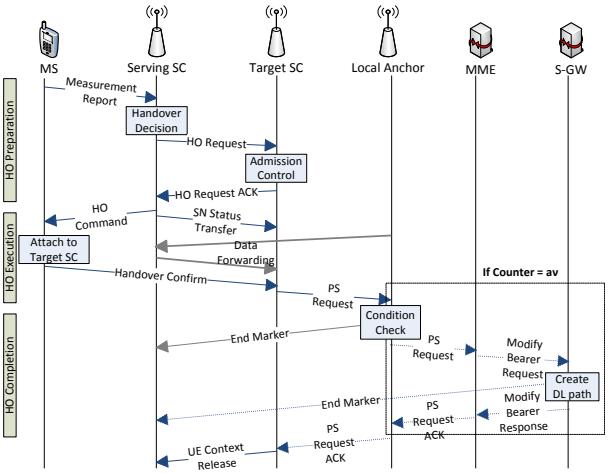

Fig. 3: LP-based handover scheme for coordinated small cells

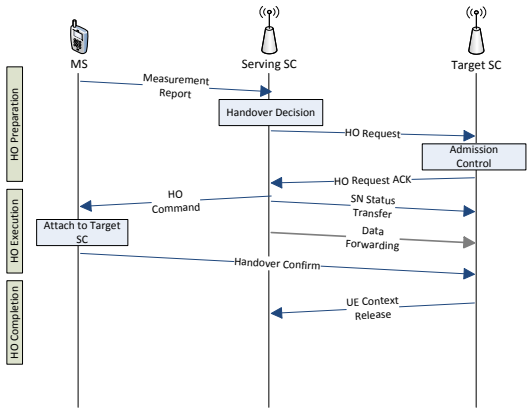

Fig. 4: DF-enhanced handover scheme

at the end of every handover, the path switch message from the target SC is not forwarded by the LA to the CN. Instead, the LA creates a new S1 path with the target SC and **updates its LART** with the new small cell endpoint address for the session. As a result, the LA forwards all future downlink data and signaling to the target SC. Following this, the LA sends an end marker to the previous SC to indicate the switching of the local path. This is continued for all further handovers for the user until the counter value equals ν, beyond which the path switch request from the latest target SC is forwarded to the CN to restore the backward key separation. The handover procedure is illustrated in Fig. 3.

D. Route Optimization-enhanced handover

The local path switching-based handover mechanism promises significant gains in terms of minimizing signaling cost, handover interruption time as well as the core network overloading. However, the data forwarding cost can be further optimized. During handover from one SC to another, the "in transit" downlink data forwarded to the target SC follows the path LA $\Rightarrow$ Serving SC $\Rightarrow$ Target SC. This, although only for the handover duration, is analogous to the **triangular routing** that takes place in mobile IP networks and results in increased data forwarding costs.

However, this is overcome by sending the path switch request message from the target SC before it has established a radio link with the MS. By doing so, the LA can already perform local path switching and establish a new S1 path with the target SC. In order to avoid any loss of in-transit packets, the target SC can indicate, in the path switch request message, the sequence number of the data (SN) or other higher layer information (delivered over the **SN status transfer message**) of the DL packets. Now, the downlink "in-transit" data is directly sent from the LA to the target SC. However, the target SC continues receiving uplink data from the serving SC's buffer. We term this mechanism as route optimization-enhanced (RO-enhanced) handover scheme. Similar to the case of LP-based handover, the RO-enhanced scheme involves sending the path switch request message to the core network every ν time the MS completes a handover for a given session.

E. Data Forwarding-enhanced handover

While the LA anchors mobility for other SCs, it is also possible that the MS is attached to the LA and needs a handover to a neighbouring SC. In this special case, it is possible to entirely eliminate the path switching operation by the target SC. Instead, the serving SC, which is the LA, performs data forwarding to the target SC using the X2 link created between LA and the target SC. When the user moves out of the target SC to another SC, the RO-enhanced handover procedure can be applied to obtain maximum savings in terms of signaling cost. The DF-enhanced handover scheme is illustrated in Fig. 4.

III. Analytical Model

In order to evaluate the performance of the handover schemes, we need to study the evolution of the user's behavior in the coordinated small cell network. To this end, we utilize discrete-time Markov model to determine the stationary probabilities of a user present in each of the small cells. In this work, we model a single cluster of small cells that also includes a local anchor small cell. Based on the obtained results, we provide closed-form expressions for different handover performance parameters.

A. Model Description

We utilize a grid topology to model a cluster of small cells as proposed in [10], [11]. The two-dimensional grid model adopted in this paper is shown in Fig. 5. Each block of the grid is an SC and is represented using the state variable S_i^j of the discrete-time Markov model. The LA (represented by S_0) is located centrally in the grid and the other small cells are deployed surrounding the local anchor in tiers. The topology consists of up to K tiers. It is constructed such that each SC has four neighboring SCs except for the SCs in the Kth tier. The number of SCs in tier i equals $4i$.

In the Markov model, we have an additional state S_{idle} indicating that there is no active session for the MS independent of which cell the user is in. The MS changes state only at the end of a discrete-time slot Δt. If the user has an active session, it can be in any of the states S_i^j where i represents the tier and j represents the index of the cell in its tier. The session arrival parameter, session duration parameter, and cell residence parameter are given by λ, μ and r. The

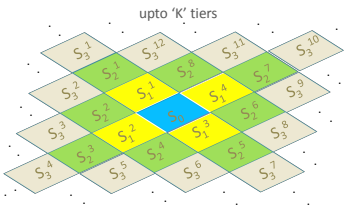

Fig. 5: Two-dimensional grid deployment model

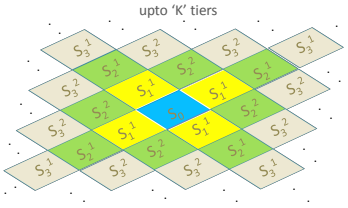

Fig. 6: Grid model after state aggregation

corresponding probabilities are P_λ, P_μ, and P_r. In this work, we consider random-walk mobility where users can move from an SC to any of its neighbors with equal probability.

In the above model, each cell is represented by a state variable. However, this may result in state space explosion, and therefore, we apply state aggregation for the Markov model making use of location symmetry and the adopted mobility model. By performing state aggregation, we have K tiers and M states in each tier where $M = \lceil (K+1)/2 \rceil$. The topology after performing state aggregation is shown in Fig. 6. The discrete-time Markov model for the aggregated states is represented in Fig. 7. Here, N represents the total number of small cells in the model, $P_{s_{ij}s_{\bar{i}\bar{j}}}$ represents the probability of the user moving from cell S_i^j to cell $S_{\bar{i}}^{\bar{j}}$ which is obtained based on the user mobility characteristics. In this work, we consider that the session arrivals follow Poisson distribution, while the cell residence time and session duration follow exponential distribution. As a result we have $P_\lambda = \lambda \Delta t$, $P_r = r\Delta t$, and $P_\mu = \mu \Delta t$.

Based on the above discrete-time Markov model, we obtain

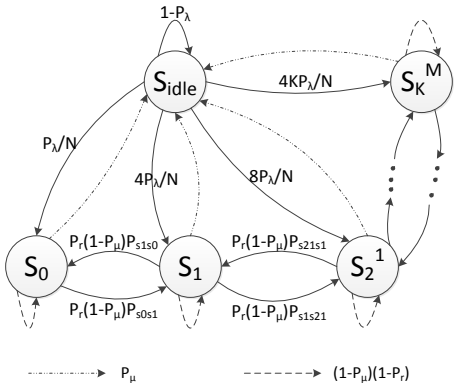

Fig. 7: Discrete-time Markov model

the stationary probability distribution of an MS in state S_i^j. Before providing the balance and normalization equations, we define the following parameters. Let $a = P_\lambda/N$, $b = (1-P_\mu)(1-P_r)$, and $d = P_r(1-P_\mu)$. In addition, we define the following parameters:

$$\{\alpha_i, \beta_i\} = \begin{cases} \{\frac{1}{2}, \frac{1}{4}\} & \text{if } i < K-1, \\ \{1,1\} & \text{if } i = K-1, \\ \{0,0\} & \text{if } i = K. \end{cases} \tag{1}$$

The balance equations are given as follows:

$$\pi_{idle} = (1-Na)\pi_{idle} + P_\mu \sum_{i=0}^{K} \sum_{j=1}^{\lceil \frac{i+1}{2} \rceil} \pi_i^j, \tag{2}$$

$$\pi_0^1 = a\pi_{idle} + b\pi_0^1 + d\beta_0\pi_1^1, \tag{3}$$

$$\pi_1^1 = 4a\pi_{idle} + b\pi_1^1 + d\Big\{\pi_0^1 + \beta_1\pi_2^1 + \alpha_1\pi_2^2\Big\}, \tag{4}$$

$$\pi_i^1 = 4a\pi_{idle} + b\pi_i^1 + d\Big\{\frac{1}{4}\pi_{i-1}^1 + \beta_i\pi_{i+1}^1 + \frac{1}{2}\alpha_i\pi_{i+1}^2\Big\}\ ;\ \forall i > 1, \tag{5}$$

$$\pi_2^2 = 4a\pi_{idle} + b\pi_2^2 + d\Big\{\frac{1}{2}\pi_1^1 + \frac{1}{2}\alpha_2\pi_3^2\Big\}, \tag{6}$$

$$\pi_3^2 = 8a\pi_{idle} + b\pi_3^2 + d\Big\{\frac{1}{2}\pi_2^1 + \frac{1}{2}\pi_2^2 + \frac{1}{2}\alpha_3\pi_4^2 + \alpha_3\pi_4^3\Big\}, \tag{7}$$

$$\pi_i^2 = 8a\pi_{idle} + b\pi_i^2 + d\Big\{\frac{1}{2}\pi_{i-1}^1 + \frac{1}{4}\pi_{i-1}^2 + \frac{1}{2}\alpha_i\pi_{i+1}^2 + \frac{1}{2}\alpha_i\pi_{i+1}^3\Big\}\ ;\ \forall i > 3, \tag{8}$$

$$\pi_{2j-2}^j = 4a\pi_{idle} + b\pi_{2j-2}^j + d\Big\{\frac{1}{4}\pi_{2j-3}^{j-1} + \frac{1}{2}\alpha_{2j-2}\pi_{2j-1}^j\Big\}\ ;\ \forall j > 2, \tag{9}$$

$$\pi_{2j-1}^j = 8a\pi_{idle} + b\pi_{2j-1}^j + d\Big\{\frac{1}{4}\pi_{2j-2}^{j-1} + \frac{1}{2}\pi_{2j-2}^j + \frac{1}{2}\alpha_{2j-1}\pi_{2j}^j + \alpha_{2j-1}\pi_{2j}^{j+1}\Big\}\ ;\ \forall j > 2, \tag{10}$$

$$\pi_i^j = 8a\pi_{idle} + b\pi_i^j + d\Big\{\frac{1}{4}\pi_{i-1}^{j-1} + \frac{1}{4}\pi_{i-1}^j + \frac{1}{2}\alpha_i\pi_{i+1}^j + \frac{1}{2}\alpha_i\pi_{i+1}^{j+1}\Big\}\ ;\ \forall j > 2, i > 2j, \tag{11}$$

where π_i^j is of the form $\pi_i^j = x_i^j\pi_{idle} + y_i^j\pi_i^j + z_i^j d\ ;\ \forall i,j$. For simplicity, in the future sections, we use the notation

$$\pi_i^j = \begin{cases} \Psi_i^j + \Omega_i^j & \forall i \neq 1, j \neq 1, \\ \Psi_i^j + \Theta_i^j + \Omega_i^j & \forall i = 1, j = 1, \end{cases} \tag{12}$$

where $\Psi_i^j = x_i^j\pi_{idle} + y_i^j\pi_i^j$, $\Theta_1^1 = d\pi_0^1$, $\Omega_i^j = z_i^j d$ and $\Omega_1^1 = z_i^j d - d\pi_0^1$.

The normalization equation is given by

$$\pi_{idle} + \sum_{i=0}^{K} \sum_{j=1}^{\lceil \frac{i+1}{2} \rceil} \pi_i^j = 1. \tag{13}$$

Using equations (2) - (11) and (13), the stationary probability distribution of the Markov model can be derived. We utilize the stationary probability distribution π_i^j and π_{idle} to derive the performance metrics.

IV. Handover Performance Metrics

The closed-form expressions for different performance characteristics are derived in this section.

A. Handover Cost

The handover cost based on the above Markov model is obtained as

$$C^{HO} = \frac{1}{\xi}\left\lfloor\frac{\xi}{\nu}\right\rfloor\Big\{\dot{C}_{01}\Omega_0^1 + \dot{C}_{11}\Theta_1^1 + \sum_{i=1}^{K}\sum_{j=1}^{\lceil\frac{K+1}{2}\rceil}\dot{C}_{ij}\Omega_i^j\Big\} + \frac{1}{\xi}\Big(\xi - \left\lfloor\frac{\xi}{\nu}\right\rfloor\Big)\Big\{\ddot{C}_{01}\Omega_0^1 + \ddot{C}_{11}\Theta_1^1 + \sum_{i=1}^{K}\sum_{j=1}^{\lceil\frac{K+1}{2}\rceil}\ddot{C}_{ij}\Omega_i^j\Big\}, \quad (14)$$

where

- ξ : Maximum number of handovers per MS per session.
- ν : Number of handovers before full path switching.
- $\dot{C}_{ij}, \ddot{C}_{ij}$: Handover costs from SC to SC in state S_i^j with full path switching and local path switching respectively.

Equation (14) is used to compute both the signaling cost C_{ij}^s and the data forwarding cost C_{ij}^D incurred during a handover.

B. Handover Interruption Time

The handover interruption time is another key performance metric for handover schemes. The closed-form expression for handover interruption time is obtained as given as

$$\tau^{HO} = \frac{1}{\xi}\left\lfloor\frac{\xi}{\nu}\right\rfloor\Big\{\dot{\tau}_{01}\Omega_0^1 + \dot{\tau}_{11}\Theta_1^1 + \sum_{i=1}^{K}\sum_{j=1}^{\lceil\frac{K+1}{2}\rceil}\dot{\tau}_{ij}\Omega_i^j\Big\} + \frac{1}{\xi}\Big(\xi - \left\lfloor\frac{\xi}{\nu}\right\rfloor\Big)\Big\{\ddot{\tau}_{01}\Omega_0^1 + \ddot{\tau}_{11}\Theta_1^1 + \sum_{i=1}^{K}\sum_{j=1}^{\lceil\frac{K+1}{2}\rceil}\ddot{\tau}_{ij}\Omega_i^j\Big\}, \quad (15)$$

where

- $\dot{\tau}_{ij}, \ddot{\tau}_{ij}$: Interruption times for handover from SC (or LA) to SC (or LA) in state S_i^j with full path switching and local path switching respectively.

C. Cost Computation

The cost functions for the proposed handover schemes are provided here. In our topology, the SC in a cluster can be connected to the LA through multi-hop using the local network. However, since the intermediary SCs only act as IP routers for the SC $\Leftrightarrow$ LA communication, the processing cost at the intermediate SCs are only accounted from the router processing cost. This cost is negligible. Similarly, the margin of link cost between single hop and multi-hop is negligible since the cluster spans only a few hundred metres. Hence, in the following cost functions, we consider the cost incurred by two small cells located at different distances from the LA incur the same cost as long as they are belong to the same cluster.

TABLE I: System Parameters

Parameter	Value	Parameter	Value
λ	$0.001/s$	C_{sc}	5ms
μ	$0.01/s$	C_{la}	10ms
r	$0.1/s$	C_{X2}	5ms
K	$1, 2, 3, 4$	C_{s1}	5ms
N	$5, 13, 25, 41$	C_{s1*}	50ms
Δt	$0.01s$	C_{scgw}	10ms

1) LP-based scheme: The signaling cost is given as

$$\ddot{C}_{ij}^s = \begin{cases} 4C_{sc} + 2C_{la} + 4C_{X2} + C_{s1}; & \text{if } i = 0, j = 1, \\ 5C_{sc} + 2C_{la} + 4C_{X2} + 2C_{s1}; & \text{if } i = 1, j = 1, \\ 5C_{sc} + 2C_{la} + 4C_{X2} + 3C_{s1}; & otherwise. \end{cases} \quad (16)$$

The data forwarding cost is given as

$$\ddot{C}_{ij}^D = \begin{cases} C_{sc} + C_{la} + C_{X2} + C_{s1}; & \text{if } i = 0, j = 1, \\ C_{sc} + C_{X2}; & \text{if } i = 1, j = 1, \\ C_{sc} + C_{la} + C_{X2} + C_{s1}; & otherwise. \end{cases} \quad (17)$$

2) RO-enhanced scheme: The signaling cost is the same as in equation (16). The data forward cost is given as

$$\ddot{C}_{ij}^D = \begin{cases} q(C_{sc} + C_{X2}) + C_{la}; & \text{if } i = 0, j = 1, \\ C_{la} + C_{s1}; & \text{if } i = 1, j = 1, \\ q(C_{sc} + C_{X2}) + (1-q)(C_{la} + C_{s1}); & otherwise, \end{cases} \quad (18)$$

where q and $1 - q$ are fractions of uplink and downlink data respectively.

3) DF-enhanced scheme: The signaling cost and data forwarding cost under DF-enhanced handover scheme differs from the RO-enhanced scheme only for the case when an MS hands over from LA to SC. These are given as $\ddot{C}_{11}^s = 4C_{sc} + 4C_{X2}$ and $\ddot{C}_{11}^D = C_{sc} + C_{X2}$.

When path switching is applied, the data forwarding cost will still be $\dot{C}_{ij}^s = \ddot{C}_{ij}^s$. However, the signaling cost is the same for all the schemes and is given by

$$\dot{C}_{ij}^s = 5C_{sc} + 4C_{X2} + 3C_{s1*} + 2C_{sc_gw} + C_{ps}. \quad (19)$$

As we see above, this is also the cost incurred in the absence of our handover schemes. Hence, we compare our solution for the case when no local path switching is utilized. In this case, we apply $\ddot{C}_{ij}^s = \dot{C}_{ij}^s$ to determine the signaling cost. Similarly the data forwarding cost is given by $\dot{C}_{ij}^D = \ddot{C}_{ij}^D = C_{sc} + C_{X2} + C_{la} + C_{s1}$.

V. Numerical Results

In this section, we numerically evaluate the proposed schemes based on the performance metrics in Section IV. The system parameter values used in this section are provided in Table I as recommended in [8]. We provide results as a ratio with respect to the current best scheme defined in the previous section. This means that a smaller ratio corresponds to improved handover performance.

In Fig. 8(a), the signaling cost ratio under the proposed handover schemes is plotted as a function of the number of tiers (K) and the number of handovers until path switching (ν). We observe that all three proposed schemes show similarity in their behavior in varying with K and ν. For small values of ν, the signaling cost ratio is large. This is because of the frequent path switching performed for each handover. However, as ν

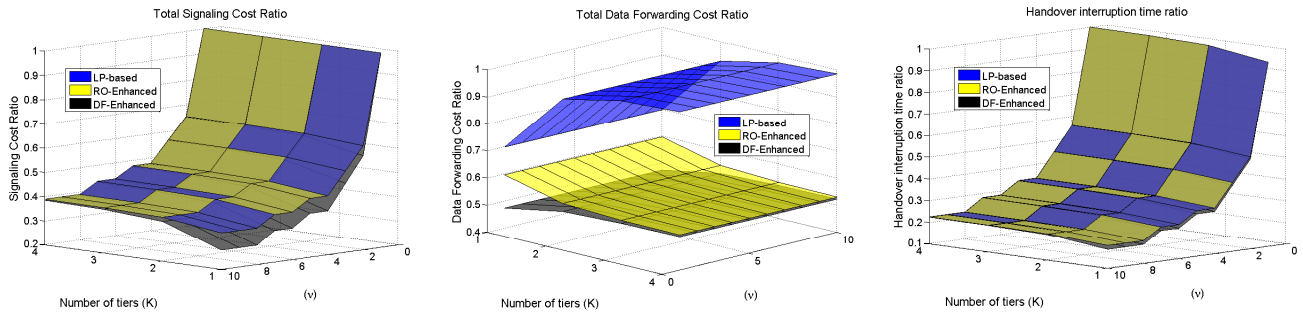

(a) (b) (c)

Fig. 8: Handover performance vs number of tiers (K) and number of handovers until path switching (ν)

increases, we observe that the signaling cost ratio decreases exponentially and reaches to around 40% of the maximum ratio. This validates our claims that minimizing the number of full path switching with the network results in signaling cost savings. The DF-enhanced scheme offers the best performance of achieving about 70% reduction in the signaling cost for $K \leq 2$ and $\nu \geq 8$. In general, all the three schemes are able to offer almost 60% signaling cost savings for $\nu = 6$. It is also interesting to note that increase in tier size (K) does not significantly affect the signaling cost performance. This allows for scalable cluster sizes as long as the network infrastructure is able to support coordination among the member SCs.

In Fig. 8(b), the total data forwarding cost ratio as a function of ν and K is plotted. It is seen that the LP-based scheme does not offer significant performance gain when $K \geq 3$. This is expected as there is a triangular routing of the "in-transit" data from the serving SC to the target SC during a handover. However, both the RO-enhanced and DF-enhanced schemes are able to achieve about 50% gain in the data forwarding cost since both the schemes enable route-optimization for the "in-transit" data packets during handover. It is interesting to note that both these schemes do not vary significantly with ν as the route-optimization does not depend on how frequently the full path switching is performed from the target SC. It is worthy of observing that the RO-enhanced scheme has a particular behavior different from the other schemes as the tier size increases. This is due to the larger costs involved when an MS hands over from LA to another SC, and with a large K, the probability of such a handover becomes very low.

In Fig. 8(c), the handover interruption time ratio is plotted against ν and K. The parameter affecting the handover interruption time is mainly the frequency of path switching. As ν increases, the path switching takes place less frequently and hence we can observe that the handover interruption time decreases and reaches a minimum of up to 20% of the maximum ratio. This corresponds to about 80% reduction in the interruption time. This is one of the key performance gains of our proposed schemes as lower interruption time reduces handover failures and enable seamless mobility for users.

VI. Conclusion

Coordination among smalls cells helps realize improved mobility management and interference management functions among others. In this work, we utilized this coordination between small cells to propose a local anchor-based handover architecture and using this, proposed novel handover schemes. For this, we developed a mathematical framework to analyze the handover schemes using Markov models. Based on this mathematical framework, we derived closed-form expressions for the key handover performance parameters. The numerical results indicate savings of about 60% in the signaling cost, about 50% in the data forwarding cost and up to 80% reduction in the handover interruption over existing schemes. The proposed framework can be utilized to analyze the performance of new handover schemes.

For future work, we intend to study and propose new handover mechanisms supporting handovers among different clusters, and to develop analytical models for such a topology. We also intend to use different probability distributions of cell residence time, session duration and session arrival time into the developed analytical model to provide a more thorough framework for studying handover mechanisms.

References

[1] 3GPP, "Evolved Universal Terrestrial Radio Access (E-UTRA); Further advancements for E-UTRA physical layer aspects," TR 36.814, Mar. 2010.

[2] ——, "Evolved Universal Terrestrial Radio Access (E-UTRA); Mobility enhancements in heterogeneous networks," TR 36.839, Dec. 2012.

[3] J. Ho and I. Akyildiz, "Local anchor scheme for reducing signaling costs in personal communications networks," *Networking, IEEE/ACM Transactions on*, vol. 4, no. 5, pp. 709 –725, oct 1996.

[4] F. Zdarsky, A. Maeder, S. Al-Sabea, and S. Schmid, "Localization of Data and Control Plane Traffic in Enterprise Femtocell Networks," in *Proc. IEEE 73rd Vehicular Technology Conference (VTC Spring)*, May 2011, pp. 1–5.

[5] A. Rath and S. Panwar, "Fast Handover in Cellular Networks with Femtocells," in *Proc. IEEE International Conference on Communications (ICC)*, Jun. 2012, pp. 2752 –2757.

[6] T. Guo, A. ul Quddus, N. Wang, and R. Tafazolli, "Local Mobility Management for Networked Femtocells Based on X2 Traffic Forwarding," *IEEE Transactions on Vehicular Technology*, vol. pp, no. 99, p. 1, 2012.

[7] 3GPP, "Evolved Universal Terrestrial Radio Access (E-UTRA) and Evolved Universal Terrestrial Radio Access Network (E-UTRAN); Overall description; Stage 2," 36.300, Mar. 2013.

[8] ——, "Feasibility study for evolved Universal Terrestrial Radio Access (UTRA) and Universal Terrestrial Radio Access Network (UTRAN)," TR 25.912, Sep. 2012.

[9] ——, "3GPP System Architecture Evolution (SAE); Security architecture," TR 33401, Mar. 2013.

[10] ——, "Evolved Universal Terrestrial Radio Access (E-UTRA); TDD Home eNode B (HeNB) Radio Frequency (RF) requirements analysis," TR 36.922, Sep. 2012.

[11] S. C. Forum, "A Small Cell Forum Whitepaper," Enterprise Femtocell Deployment Guidelines, Tech. Rep., Feb. 2012.